

DO-TH 2000/13

hep-ph/0009348

September 2000

# Has the QCD RG-Improved Parton Content of Virtual Photons been Observed?

M. Glück, E. Reya, I. Schienbein

*Institut für Physik, Universität Dortmund  
D-44221 Dortmund, Germany*

## Abstract

It is demonstrated that present  $e^+e^-$  and DIS ep data on the structure of the virtual photon can be understood entirely in terms of the standard 'naive' quark-parton model box approach. Thus the QCD renormalization group (RG) improved parton distributions of virtual photons, in particular their gluonic component, have not yet been observed. The appropriate kinematical regions for their future observation are pointed out as well as suitable measurements which may demonstrate their relevance.

# 1 Introduction

Recent measurements and experimental studies of dijet events in deep inelastic  $ep$  [1] and of double-tagged  $e^+e^-$  [2] reactions have indicated a necessity for assigning a (QCD resummed) parton content of virtual photons  $\gamma(P^2)$  as suggested and predicted theoretically [3 – 9]. In particular the DIS dijet production data [1] appear to imply a sizeable gluon component  $g^{\gamma(P^2)}(x, Q^2)$  in the derived effective parton density of the virtual photon, where  $Q^2$  refers to the hadronic scale of the process,  $Q \sim p_T^{\text{jet}}$ , or to the virtuality of the probe photon  $\gamma^*(Q^2)$  which probes the virtual target photon  $\gamma(P^2)$  in  $e^+e^- \rightarrow e^+e^-X$ . It is the main purpose of this article to demonstrate that this is not the case and that all present data on virtual photons can be explained entirely in terms of the conventional QED doubly-virtual box contribution  $\gamma^*(Q^2)\gamma(P^2) \rightarrow q\bar{q}$  in fixed order perturbation theory – sometimes also referred to as the quark-parton model (QPM).

This is of course in contrast to the well known case of a real photon  $\gamma \equiv \gamma(P^2 \equiv 0)$  whose (anti)quark and gluon content has been already experimentally established (for recent reviews see [10, 11]) which result mainly from resummations (inhomogeneous evolutions) of the pointlike mass singularities proportional to  $\ln Q^2/m_q^2$  occurring in the box diagram of  $\gamma^*(Q^2)\gamma \rightarrow q\bar{q}$  for the light  $q = u, d, s$  quarks. This is in contrast to a virtual photon target where  $\gamma^*(Q^2)\gamma(P^2) \rightarrow q\bar{q}$  does not give rise to collinear (mass) singularities but instead just to finite contributions proportional to  $\ln Q^2/P^2$  which a priori need not be resummed to all orders in QCD.

In Section 2 we shall present the usual QED box contributions to the virtual photon structure functions and summarize in the Appendix the rather involved exact results in a compact form which include all  $P^2/Q^2$  as well as  $m_q^2/Q^2$  contributions, since the latter ones are also important for heavy quark ( $c, b, t$ ) production. In Sec. 3 we recapitulate briefly how these results are resummed in QCD and how (anti)quark and gluon distributions in virtual photons are modeled and generated in QCD, while Sec. 4 contains a comparison

with present  $e^+e^-$  and DIS ep data. Suggestions of experimental signatures which can probe the QCD parton content, in particular the gluon content of virtual photons are presented in Sec. 5 and our conclusions are finally drawn in Section 6.

## 2 Virtual Photon Structure Functions and the QED Box Contributions

The virtual photon structure functions arising in the process  $e^+(p_1)e^-(p_2) \rightarrow e^+(p_1')e^-(p_2') + \text{hadrons}$  are specified by the kinematical variables  $q = p_1 - p_1'$ ,  $p = p_2 - p_2'$ ,  $Q^2 = -q^2$ ,  $P^2 = -p^2$ ,  $y_1 = q \cdot p / p_1 \cdot p$  and  $y_2 = p \cdot q / p_2 \cdot q$ . The Bjorken limit is given by  $P^2 \ll Q^2$ , i.e. the virtuality of the target photon being small as compared to the one of the probe photon, and the corresponding Bjorken variable is  $x = Q^2 / 2p \cdot q$  where  $0 \leq x \leq (1 + P^2/Q^2)^{-1}$ . The physically measured effective structure function in the Bjorken limit is [12, 13, 11]

$$\frac{1}{x} F_{\text{eff}}(x; Q^2, y_1; P^2, y_2) = F_{\text{TT}} + \varepsilon(y_1)F_{\text{LT}} + \varepsilon(y_2)F_{\text{TL}} + \varepsilon(y_1)\varepsilon(y_2)F_{\text{LL}}, \quad (2.1)$$

where T and L refer to the transverse and longitudinal polarization, respectively, of the probe and target photons, and  $\varepsilon(y_i)$  are the ratios of longitudinal to transverse photon fluxes,

$$\varepsilon(y_i) = 2(1 - y_i)/[1 + (1 - y_i)^2], \quad (2.2)$$

and where furthermore  $F_{ab} = F_{ab}(x, Q^2, P^2)$  with  $a = (\text{L}, \text{T})$ ,  $b = (\text{L}, \text{T})$ . In the following we shall consider the kinematical region  $y_i \ll 1$  relevant for double-tag experiments [2, 14] performed thus far. Thus eq. (2.1) reduces to

$$\frac{1}{x} F_{\text{eff}}(x, Q^2, P^2) \simeq F_{\text{TT}} + F_{\text{LT}} + F_{\text{TL}} + F_{\text{LL}} \quad (2.3)$$

and usually one defines [11, 12, 13]

$$\begin{aligned} \frac{1}{x} F_2 &= F_{\text{TT}} + F_{\text{LT}} - \frac{1}{2}(F_{\text{TL}} + F_{\text{LL}}) \\ 2F_1 &\equiv 2F_{\text{T}} = \bar{\beta}^2(F_{\text{TT}} - \frac{1}{2}F_{\text{TL}}) \end{aligned} \quad (2.4)$$

where  $\bar{\beta}^2 = 1 - 4x^2 P^2 / Q^2$ , and  $F_L = \bar{\beta}^2 F_2 - 2x F_1$ . (Note that the  $F_{ab}$  are normalized with respect to  $\frac{1}{x} F_2$ , i.e.  $F_{ab} \equiv (Q^2 / 4\pi^2 \alpha) (x\bar{\beta})^{-1} \sigma_{ab}$  with  $\sigma_{ab}$  denoting the directly measurable cross sections.) So far, our results are entirely general.

We shall furthermore introduce the decomposition

$$F_{ab} = F_{ab}^\ell + F_{ab}^h \quad (2.5)$$

with  $F_{ab}^{\ell(h)}$  denoting the light quark  $q = u, d, s$  (heavy quark  $h = c, b, t$ ) contributions, respectively. The relevant (QPM) expressions of the fully virtual ( $P^2 \neq 0$ ) box for  $F_{ab}$  are summarized in the Appendix: The light  $u, d, s$  contributions to  $F_{ab}^\ell$  are obtained from eqs. (A.1) – (A.4) by setting  $m \equiv m_q = 0$  ( $\lambda = 0$ ) and summing over  $q = u, d, s$ . (Note that the box expressions involving a real photon,  $\gamma^*(Q^2) \gamma(P^2 = 0) \rightarrow q\bar{q}$ , require on the contrary a finite regulator mass  $m \equiv m_q \neq 0$ ; here one usually chooses  $m_q$  to be, somewhat inconsistently, a constant, i.e.  $Q^2$ -independent effective constituent mass,  $m_q \simeq 0.3$  GeV.) For each heavy quark flavor  $h = c, b, t$  the heavy contribution  $F_{ab}^h$  in (2.5) is obtained from (A.1) – (A.4) with  $e_q \equiv e_h$  and  $m \equiv m_h$ . Only charm gives a non-negligible contribution for which we choose  $m_c = 1.4$  GeV throughout.

Finally, it is instructive to recall the asymptotic results of our virtual ( $P^2 \neq 0$ ) box expressions for the light  $q = u, d, s$  quarks derived from (A.1) – (A.4) in the Bjorken limit  $P^2 / Q^2 \ll 1$ :

$$\begin{aligned} F_{\text{TT}}^\ell &\simeq 3(\Sigma e_q^4) \frac{\alpha}{\pi} \left\{ [x^2 + (1-x)^2] \ln \frac{Q^2}{P^2 x^2} + 4x(1-x) - 2 \right\} \\ F_{\text{LT}}^\ell &\simeq F_{\text{TL}}^\ell \simeq 3(\Sigma e_q^4) \frac{\alpha}{\pi} 4x(1-x) \\ F_{\text{LL}}^\ell &\simeq 0, \end{aligned} \quad (2.6)$$

i.e. using (2.4),

$$\frac{1}{x} F_{2, \text{box}}^\ell(x, Q^2, P^2) \simeq 3(\Sigma e_q^4) \frac{\alpha}{\pi} \left\{ [x^2 + (1-x)^2] \ln \frac{Q^2}{P^2 x^2} + 6x(1-x) - 2 \right\}. \quad (2.7)$$

In this limit  $F_{\text{eff}}^\ell$  in(2.3) reduces to

$$\frac{1}{x} F_{\text{eff}}^{\ell, \text{box}}(x, Q^2, P^2) \simeq \frac{1}{x} F_{2, \text{box}}^\ell + \frac{3}{2} F_{\text{LT}}^\ell. \quad (2.8)$$

Such a relation holds for the heavy quark contribution  $F_{\text{eff}}^{h, \text{box}}$  in the Bjorken limit as well, since also  $F_{\text{LL}}^h$  in (A.4) for  $m \equiv m_h \neq 0$  becomes vanishingly small for  $P^2 \ll Q^2$ .

The universal process independent part of the pointlike box expressions in (2.6) and (2.7) proportional to  $\ln Q^2/P^2$  may be used to define formally, as in the case of a real photon target [15], light (anti)quark distributions in the virtual photon  $\gamma(P^2)$ :

$$\frac{1}{x} F_{2, \text{box}}^\ell(x, Q^2, P^2)|_{\text{univ.}} = F_{\text{TT}}^\ell|_{\text{univ.}} \equiv \sum_{q=u, d, s} e_q^2 \left[ q_{\text{box}}^{\gamma(P^2)}(x, Q^2) + \bar{q}_{\text{box}}^{\gamma(P^2)}(x, Q^2) \right] \quad (2.9)$$

with

$$q_{\text{box}}^{\gamma(P^2)}(x, Q^2) = \bar{q}_{\text{box}}^{\gamma(P^2)}(x, Q^2) = 3e_q^2 \frac{\alpha}{2\pi} [x^2 + (1-x)^2] \ln \frac{Q^2}{P^2}. \quad (2.10)$$

It should be noted that these naive, i.e. not QCD resummed, box expressions do not imply a gluon component in the virtual photon,  $g_{\text{box}}^{\gamma(P^2)}(x, Q^2) = 0$ .

### 3 The QCD Parton Content of Virtual Photons

Deep inelastic scattering (DIS) involving virtual photons,  $\gamma(P^2)$ , is somewhat problematic since it turns out that the implementation of the physical continuity requirement at  $P^2 = 0$  is nontrivial at the next-to-leading order (NLO) level due to kinematical discontinuities at this point, as exemplified for example by the different expressions in eqs. (2.7) and (A.6). A solution to this problem was proposed in [9] where part of these discontinuities were smoothed out in the construction of the photonic parton distributions  $f^{\gamma(P^2)}(x, Q^2)$  ( $f = q, \bar{q}, g$  with  $q = u, d, s$ ) and where the remaining NLO discontinuities, related to the ‘direct’ contributions, were eliminated by calculating these contributions as if  $P^2 = 0$ . Thus whenever these virtual photons, with their virtuality being here entirely taken care of by the ‘equivalent photon’ flux factors [9, 12, 16], are probed at a scale  $Q^2 \gg P^2$  they

should be considered as real photons which means that cross sections (Wilson coefficient functions) of partonic subprocesses involving  $\gamma(P^2)$  should be calculated as if  $P^2 = 0$ . It should be stressed that this procedure is not a free option but a necessary consistency condition for introducing the concept of the resolved parton content of the virtual photon as an alternative to a non-resummed fixed order perturbative analysis at  $P^2 \neq 0$  as, for example, the QED box results discussed in the previous Section. This consistency requirement is related to the fact that all the resolved contributions due to  $q^{\gamma(P^2)}(x, Q^2) = \bar{q}^{\gamma(P^2)}(x, Q^2)$  and  $g^{\gamma(P^2)}(x, Q^2)$  are calculated (evolved) as if these partons are massless [3–7, 9], i.e. employing photon splitting functions for real photons, etc., despite of the fact that their actual virtuality is given by  $P^2 \neq 0$ .

This rule implies, for example, that the NLO ‘direct’ contribution  $C_{\gamma(P^2)}(x)$  to  $F_2(x, Q^2, P^2)$  has to be the same  $C_\gamma(x)$  as for real photons, i.e. has to be inferred from eq. (A.6) of the real (target) photon subprocess  $\gamma^*(Q^2)\gamma \rightarrow q\bar{q}$ , and not from eq. (2.7) which derives from the doubly virtual box  $\gamma^*(Q^2)\gamma(P^2) \rightarrow q\bar{q}$  as originally proposed [3, 4]. Thus for the light  $u, d, s$  flavors we have [9]

$$\frac{1}{x} F_2^\ell(x, Q^2, P^2) = 2 \sum_{q=u,d,s} e_q^2 \left\{ q^{\gamma(P^2)}(x, Q^2) + \frac{\alpha_s(Q^2)}{2\pi} [C_q \otimes q^{\gamma(P^2)} + C_g \otimes g^{\gamma(P^2)}] \right\} \quad (3.1)$$

with the usual (on-shell) Wilson coefficients  $C_{q,g}(x)$  as given, for example, in [9] and the ‘direct’  $C_\gamma(x) = [3/(1/2)]C_g(x)$  contribution has already been absorbed into the definition of  $q^{\gamma(P^2)}(x, Q^2)$  which thus refer to the DIS $_\gamma$  factorization scheme (see, e.g., eq. (4) in [9]). The heavy quark (predominantly charm) contribution to  $F_2$  in (2.5) is given by

$$F_2^h(x, Q^2, P^2) = F_{2,\text{box}}^h + F_{2,g^{\gamma(P^2)}}^h \quad (3.2)$$

with the ‘direct’ box contribution given by eq. (A.7) and the ‘resolved’ contribution by

$$F_{2,g^{\gamma(P^2)}}^h(x, Q^2) = \int_{z_{\min}}^1 \frac{dz}{z} z g^{\gamma(P^2)}(z, \mu_F^2) f_2^{\gamma^*(Q^2)g^{\gamma \rightarrow h\bar{h}}}\left(\frac{x}{z}, Q^2\right) \quad (3.3)$$

where  $\frac{1}{x} f_2^{\gamma^*(Q^2)g^{\gamma \rightarrow h\bar{h}}}(x, Q^2)$  is given by eq. (A.7) with  $e_h^4 \alpha \rightarrow e_h^2 \alpha_s(\mu_F^2)/6$ ,  $z_{\min} = x(1 + 4m_h^2/Q^2)$  and  $\mu_F^2 \simeq 4m_h^2$ . Furthermore, since an effectively real photon has no longitudinal

components ( $F_{\text{TL}}, F_{\text{LL}}$ ) we have, instead of (2.3) or (2.8),

$$F_{\text{eff}}(x, Q^2, P^2) = F_2(x, Q^2, P^2). \quad (3.4)$$

Finally it should be remarked that the parton distributions  $f^\gamma(x, Q^2)$  of a real photon can be calculated in a parameter-free way [9] by employing a coherent superposition of vector mesons, which maximally enhances  $u$ -quark contributions to  $F_2^\gamma$ , for determining the hadronic input  $f_{\text{had}}^\gamma(x, Q_0^2)$  at a GRV-like [17] input scale  $Q_0^2 \equiv \mu^2 \simeq 0.3 \text{ GeV}^2$ . For a virtual photon, however, an additional assumption is needed about the  $P^2$ -dependence of the hadronic input distributions of a virtual photon,  $f_{\text{had}}^{\gamma(P^2)}(x, Q_0^2)$ , which is commonly assumed [6, 7, 9] to be represented by a vector-meson-propagator-inspired suppression factor  $\eta(P^2) = (1 + P^2/m_\rho^2)^{-2}$  with  $m_\rho^2 = 0.59 \text{ GeV}^2$ . Thus our above consistency requirement affords furthermore the following boundary conditions for quarks and gluons [9]:

$$f^{\gamma(P^2)}(x, Q^2 = \tilde{P}^2) = f_{\text{had}}^{\gamma(P^2)}(x, \tilde{P}^2) = \eta(P^2) f_{\text{had}}^\gamma(x, \tilde{P}^2) \quad (3.5)$$

in LO as well as in NLO of QCD, where  $\tilde{P}^2 = \max(P^2, \mu^2)$  as dictated by continuity in  $P^2$  as well as by the fact that the hadronic component of  $f^{\gamma(P^2)}(x, Q^2)$  is probed at the scale  $Q^2 = \tilde{P}^2$  [5, 6, 7, 9] where the pointlike component vanishes by definition. The second equality in (3.5) follows from the consistency requirement that  $C_{\gamma(P^2)}(x)$  is taken to be given by  $C_\gamma(x)$  and consequently the application of the same  $\overline{\text{MS}} \rightarrow \text{DIS}_\gamma$  factorization scheme transformation as for the real photon [9]. Thus the resulting perturbatively stable LO and NLO parton densities  $f^{\gamma(P^2)}(x, Q^2)$  are smooth in  $P^2$  and apply to all  $P^2 \geq 0$  whenever  $\gamma(P^2)$  is probed at scales  $Q^2 \gg P^2$ .

A different approach has been suggested by Schuler and Sjöstrand [7]. Apart from using somewhat different input scales  $Q_0$  and parton densities, the perturbatively exactly calculable box expressions for  $\Lambda^2 \ll P^2 \ll Q^2$  in (2.6) and (2.7) are, together with their LO-QCD  $Q^2$ -evolutions, extrapolated to the case of real photons  $P^2 = 0$  by employing some dispersion-integral-like relations. These link perturbative and non-perturbative

contributions and allow a smooth limit  $P^2 \rightarrow 0$ . (Note, however, that the LO  $Q^2$ -evolutions are performed by using again the splitting functions of real photons and on-shell partons.) Since one works here explicitly with virtual ( $P^2 \neq 0$ ) expressions, the longitudinal contributions of the virtual photon target should be also taken into account when calculating  $F_{\text{eff}} = F_2 + \frac{3}{2}F_{\text{LT}}$  similarly to (2.8), as described for example in [6], which is in contrast to our approach in (3.4).

In an alternative approach [18] one may consider the longitudinal component of the virtual photon target  $\gamma_{\text{L}}(P^2)$  to possess, like the transverse component, a universal process independent hadronic content obtained radiatively via the standard homogeneous (Altarelli-Parisi)  $Q^2$ -evolution equations with the boundary conditions for the pointlike component at  $Q^2 = P^2$  given by  $F_{\text{TL}}^\ell$  in eq. (2.6) for quarks together with a vanishing gluonic input in LO. We have checked that the predictions for  $F_{\text{eff}}(x, Q^2, P^2)$  obtained in this approach differ only slightly (typically about 10% or less) from those of the standard fixed order perturbative approach at presently relevant kinematical regions ( $P^2 \lesssim \frac{1}{10}Q^2$ ,  $x \gtrsim 0.05$ ) due to the smallness of  $F_{\text{TL}}^\ell$  relative to  $F_{\text{TT}}^\ell$  in (2.6).

As already mentioned, at  $Q^2 \gg P^2 \gg \Lambda^2$ , the  $\ln Q^2/P^2$  terms in (2.6) and (2.7) need not necessarily be resummed in contrast to the situation for the real photon ( $P^2 = 0$ ) with its well known mass singularities  $\ln Q^2/m_q^2$  in (A.6) which afford the introduction of scale dependent (RG-improved) parton distributions which are a priori unknown unless one resorts to some model assumptions about their shape at some low resolution scale (see, e.g., [9] and the recent reviews [10, 11]).



## 4 Comparison of Theoretical Expectations with Present $e^+e^-$ Virtual Photon Data

We shall now turn to a quantitative study of the various QED-box and QCD  $Q^2$ -evolved structure function expectations for a virtual photon target and confront them with all presently available  $e^+e^-$  data of PLUTO [14] and the recent one of LEP-L3 [2]. Despite the limited statistics of present data the box predictions for  $F_{\text{eff}}$  in (2.3) shown in figs. 1 and 2 appear to be in even better agreement with present measurements than the QCD resummed expectations of SaS [7] and GRS [9]. Typical QCD effects like the increase in the small-x region in fig. 1, being partly caused by the presence of a finite gluon content  $g^{\gamma(P^2)}(x, Q^2)$ , cannot be delineated with the present poor statistics data.

These results clearly demonstrate that the naive QPM predictions derived from the doubly-virtual box  $\gamma^*(Q^2)\gamma(P^2) \rightarrow q\bar{q}$  fully reproduce all  $e^+e^-$  data on the structure of virtual photons  $\gamma(P^2)$ . In other words, there is no sign of a QCD resummed parton content in virtual photons in present data, in particular of a finite gluon content  $g^{\gamma(P^2)}(x, Q^2)$  which is absent in the ‘naive’ box (QPM) approach.

Characteristic possible signatures for QCD effects which are caused by the presence of a finite and dominant gluon component  $g^{\gamma(P^2)}$  will be discussed in Sec. 6.

## 5 Comparison of Theoretical Expectations with DIS ep Data and Effective Quark Distributions of Virtual Photons

In order to extract the parton densities of virtual photons from DIS ep dijet data, the H1 collaboration [1] has adopted the ‘single effective subprocess approximation’ [19] which exploits the fact that the dominant contributions to the cross section in LO-QCD comes

from the  $2 \rightarrow 2$  parton-parton hard scattering subprocesses that have similar shapes and thus differ mainly by their associated color factors. Therefore the sum over the partonic subprocesses can be replaced by a single effective subprocess cross section and effective parton densities for the virtual photon given by

$$\tilde{f}^{\gamma(P^2)}(x, Q^2) = \sum_{q=u, d, s} \left[ q^{\gamma(P^2)}(x, Q^2) + \bar{q}^{\gamma(P^2)}(x, Q^2) \right] + \frac{9}{4} g^{\gamma(P^2)}(x, Q^2) \quad (5.1)$$

with a similar relation for the proton  $\tilde{f}^P(x, Q^2)$  which is assumed to be known. It should be emphasized that such an effective procedure does not hold in NLO where all additional (very different)  $2 \rightarrow 3$  subprocesses contribute [20]. This NLO analysis affords therefore a confrontation with more detailed data on the triple-differential dijet cross-section as compared to presently available data [1] which are not yet sufficient for examining the relative contributions of  $q^{\gamma(P^2)}(x, Q^2)$  and  $g^{\gamma(P^2)}(x, Q^2)$ . In fig. 3 we compare our LO RG-resummed predictions for  $\tilde{f}^{\gamma(P^2)}(x, Q^2)$  with the naive non-resummed universal (process independent) box expressions in (2.10). Although the fully QCD-resummed results are sizeable and somewhat larger in the small  $P^2$  region than the universal box expectations, present H1 data [1] at  $Q^2 \equiv (p_T^{\text{jet}})^2 = 85 \text{ GeV}^2$  cannot definitely distinguish between these predictions. It should be furthermore noted that the QCD gluon contribution  $g^{\gamma(P^2)}(x, Q^2)$  is suppressed at the large values of  $x$  shown in fig. 3. Therefore present data [1] cannot discriminate between the finite QCD resummed component  $g^{\gamma(P^2)}(x, Q^2)$  and the non-resummed  $g_{\text{box}}^{\gamma(P^2)}(x, Q^2) = 0$ .

It is obvious that these two results shown in fig. 3 are only appropriate for virtualities  $P^2 \ll Q^2$ , typically  $P^2 = 10$  to  $20 \text{ GeV}^2$  at  $Q^2 = 85 \text{ GeV}^2$ , since  $\mathcal{O}(P^2/Q^2)$  contributions are neglected in RG-resummations as well as in the definition (2.10). In order to demonstrate the importance of  $\mathcal{O}(P^2/Q^2)$  power corrections in the large  $P^2$  region let us define, generalizing the definition (2.9), some effective (anti)quark distributions as common via

$$\frac{1}{x} F_{2, \text{box}}^\ell(x, Q^2, P^2) \equiv \sum_{q=u, d, s} e_q^2 \left[ q_{\text{eff}}^{\gamma(P^2)}(x, Q^2) + \bar{q}_{\text{eff}}^{\gamma(P^2)}(x, Q^2) \right] \quad (5.2)$$

where, of course,  $q_{\text{eff}}^{\gamma(P^2)} = \bar{q}_{\text{eff}}^{\gamma(P^2)}$  and the full box expression for  $F_{2,\text{box}}^\ell$  in (2.4) for light quarks is given in (A.1) – (A.4) with  $m \equiv m_q = 0$ , i.e.  $\lambda = 0$ . The full box expressions imply again  $g_{\text{eff}}^{\gamma(P^2)}(x, Q^2) = 0$  in contrast to the QCD resummed gluon distribution. The  $q_{\text{eff}}^{\gamma(P^2)}$  introduced in (5.2) is, in contrast to (2.9), of course non-universal. The ‘effective’ results shown in fig. 3 clearly demonstrate the importance of the  $\mathcal{O}(P^2/Q^2)$  terms at larger values of  $P^2 \lesssim Q^2$  which are not taken into account by the QCD resummations and by the universal box expressions in (2.10) also shown in fig. 3. It is interesting that the non-universal  $q_{\text{eff}}^{\gamma(P^2)}$  defined via  $F_2$  in (5.2) describes the H1-data at large values of  $P^2$  in fig. 3 remarkably well. This may be accidental and it remains to be seen whether future LO analyses will indicate the general relevance of  $q_{\text{eff}}^{\gamma(P^2)}(x, Q^2)$  in the large  $P^2$  region.

As we have seen, present DIS dijet data cannot discriminate between the universal naive box and QCD-resummed expectations in the theoretically relevant region  $P^2 \ll Q^2$ , mainly because these data are insensitive to the gluon content in  $\gamma(P^2)$  generated by QCD-evolutions which is absent within the naive box approach. Therefore we finally turn to a brief discussion where such typical QCD effects may be observed and delineated by future experiments.

## 6 Possible Signatures for the QCD Parton Content of Virtual Photons

Since  $e^+e^-$  and DIS ep dijet data cannot, at present, delineate the QCD-resummed parton content of a virtual photon, in particular not its gluon content, we shall now propose and discuss a few cases where such typical QCD effects may be observed and possibly confirmed by future experiments.

Charm production in  $e^+e^- \rightarrow e^+e^- c\bar{c}X$  would be a classical possibility to delineate such effects due to a nonvanishing  $g^{\gamma(P^2)}(x, Q^2)$ . In fig. 4 we compare the usual (fixed

order) ‘direct’ box contribution to  $F_2^c$  with the ‘resolved’ gluon–initiated one in (3.2), as given by (3.3). The ‘direct’ box contribution entirely dominates in the large  $x$  region,  $x \gtrsim 0.05$ , accessible by present experiments (cf. figs. 1 and 2), whereas the typical QCD–resummed ‘resolved’ contribution becomes comparable to the ‘direct’ one and eventually dominates in the small  $x$  region,  $x < 0.05$ . Thus a careful measurement of the charm contribution to  $F_2$  at  $x \lesssim 0.05$  would shed some light on the QCD parton (gluon) content of virtual photons, since such a ‘resolved’ contribution in fig. 4 would be absent within the naive box approach.

The effective parton distribution  $\tilde{f}^{\gamma(P^2)}(x, Q^2)$  in (5.1) at not too large values of  $x$  and  $P^2$ , as may be extracted in LO from DIS ep dijet data, would be another possibility to observe QCD–resummation effects due to a nonvanishing gluon component  $g^{\gamma(P^2)}(x, Q^2)$ . In fig. 5 we show the quark and gluon contributions to  $\tilde{f}^{\gamma(P^2)}$  in (5.1) separately. The box (anti)quark contributions, which are similar to the QCD–resummed ones, entirely dominate over the QCD–resummed gluon contribution in the large  $x$  region,  $x \gtrsim 0.4$ , accessible to present experiments (cf. fig. 3). Only below  $x \simeq 0.3$  does the QCD gluon contribution become comparable to the (anti)quark components and dominates, as usual, for  $x \lesssim 0.1$ . It should be remembered that  $g_{\text{box}}^{\gamma(P^2)}(x, Q^2) = 0$ . Furthermore, the increase of the RG–resummed  $q^{\gamma(P^2)}(x, Q^2)$  at small  $x$  in fig. 5 is induced by the vector–meson–dominance–like input for the  $Q^2$ –evolution of the ‘hadronic’ component of photon’s parton distribution [7, 9] and is disregarded in our naive box (QPM) analysis.

Thus a measurement of dijets produced in DIS ep reactions in the not too large  $x$  region,  $x \lesssim 0.3$ , would probe the QCD parton content of virtual photons, in particular their gluon content which is absent in the naive QPM box approach. In this region, and at not too large photon virtualities  $P^2 \lesssim 5 \text{ GeV}^2$  shown in fig. 5, the ‘resolved’ gluon–dominated contribution of the virtual photon to high  $E_T$  jet production at scales  $Q \equiv E_T \simeq 5 - 10 \text{ GeV}$  exceeds by far the ‘direct’ box–like contribution of a pointlike virtual photon [21].

## 7 Summary and Conclusions

Virtual photons  $\gamma(P^2)$ , probed at a large scale  $Q^2 \gg P^2$ , may be described either by fixed-order perturbation theory, which in lowest order of QCD yield the quarks and antiquarks generated by the universal part of the ‘box’ diagram, or alternatively by their renormalization group (RG) improved counterparts including particularly the gluon distribution  $g^{\gamma(P^2)}(x, Q^2)$ .

The results in Sections 3 and 4 demonstrate that all presently available  $e^+e^-$  and DIS ep dijet data can be fully accounted for by the standard doubly-virtual QED box diagram and are not yet sensitive to RG resummation effects which are manifest only in the presently unexplored low- $x$  region of the parton distributions in  $\gamma(P^2)$ . In fact, as shown in Section 6, these resummation effects start to dominate only a  $x < 0.3$  and may be observed by future measurements at  $P^2 = \mathcal{O}(1 \text{ GeV}^2)$  of  $\sigma(ep \rightarrow e jjX)$  or  $\sigma(e^+e^- \rightarrow e^+e^- c\bar{c}X)$  at high energy collisions. These measurements could finally discriminate between the fixed order and RG-improved parton distributions of the virtual photon.

## Appendix

The most general QPM box–results for  $F_{ab}$  appearing in the structure function relations (2.3) and (2.4) derive from the fully off–shell QED box–diagram  $\gamma^*(Q^2)\gamma(P^2) \rightarrow q\bar{q}$  for each quark flavor with charge  $e_q$ , carrying 3 colors and by keeping the quark mass  $m$  as well [12, 4]. These results can be conveniently written as :

$$\begin{aligned}
F_{\text{TT}} = & 3 e_q^4 \frac{\alpha}{\pi} \theta(\beta^2) \frac{1}{\beta^5} \left\{ \left[ 1 - 2x(1-x) - 2\delta(1-\delta) - 4x\delta(x^2 + \delta^2) + 8x^2\delta^2 \right. \right. \\
& \left. \left[ 1 + (1-x-\delta)^2 \right] + \lambda\bar{\beta}^2(1-x-\delta)^2 - \frac{1}{2}\lambda^2\bar{\beta}^4(1-x-\delta)^2 \right] \ln \frac{\beta_+}{\beta_-} \\
& + \beta\bar{\beta} \left[ 4x(1-x) - 1 + 4\delta(1-\delta) - 8x\delta(1-x^2 - \delta^2) \right. \\
& \left. \left. - (4x\delta + \lambda\bar{\beta}^2)(1-x-\delta)^2 - \frac{4x\delta\bar{\beta}^4}{4x\delta + \lambda\bar{\beta}^2} \right] \right\} \quad (\text{A.1})
\end{aligned}$$

$$\begin{aligned}
F_{\text{LT}} = & 3 e_q^4 \frac{\alpha}{\pi} \theta(\beta^2) \frac{4}{\beta^5} (1-x-\delta) \left\{ x \left[ -\frac{1}{2}\lambda\bar{\beta}^2(1-2\delta(1+x-\delta)) \right. \right. \\
& \left. \left. - 2\delta(-1+2x+2\delta-2x\delta(1+x+\delta)) \right] \ln \frac{\beta_+}{\beta_-} \right. \\
& \left. + \beta\bar{\beta} \left[ x(1-6\delta+6\delta^2+2x\delta) + \delta\bar{\beta}^2 \frac{4x\delta}{4x\delta + \lambda\bar{\beta}^2} \right] \right\} \quad (\text{A.2})
\end{aligned}$$

$$F_{\text{TL}} = F_{\text{LT}} [x \leftrightarrow \delta] \quad (\text{A.3})$$

$$F_{\text{LL}} = 3 e_q^4 \frac{\alpha}{\pi} \theta(\beta^2) \frac{16}{\beta^5} \delta x (1-x-\delta)^2 \left\{ (1+2x\delta) \ln \frac{\beta_+}{\beta_-} - 2\beta\bar{\beta} \frac{6x\delta + \lambda\bar{\beta}^2}{4x\delta + \lambda\bar{\beta}^2} \right\} \quad (\text{A.4})$$

where  $\delta = xP^2/Q^2$ ,  $\lambda = 4m^2/W^2$  with  $W^2 = Q^2(1-x-\delta)/x \geq (2m)^2$ , and  $\beta^2 = 1 - \lambda$ ,  $\bar{\beta}^2 = 1 - 4x\delta$ ,  $\beta_{\pm} = 1 \pm \beta\bar{\beta}$ . The relevant asymptotic expressions for the light  $q = u, d, s$  quark ( $m \equiv m_q = 0$ , i.e.,  $\lambda = 0$ ) contributions in the Bjorken limit  $P^2 \ll Q^2$  are given in eq. (2.6).

For completeness it should be noted that the general virtual box results in (A.1) – (A.4)

reduce for  $P^2 = 0$  ( $\delta = 0$ ) to the standard box–diagram  $\gamma^*(Q^2) \gamma \rightarrow q\bar{q}$  expressions for a real photon  $\gamma \equiv \gamma(P^2 = 0)$  : in the light quark sector where  $\lambda \ll 1$ , i.e.  $m^2 \equiv m_q^2 \ll Q^2$ , we have

$$\begin{aligned} F_{\text{TT}}^\ell &= 3 \Sigma e_q^4 \frac{\alpha}{\pi} \left\{ [x^2 + (1-x)^2] \ln \frac{Q^2(1-x)}{m_q^2 x} + 4x(1-x) - 1 \right\} \\ F_{\text{LT}}^\ell &\simeq 3 \Sigma e_q^4 \frac{\alpha}{\pi} 4x(1-x) \\ F_{\text{TL}}^\ell &= F_{\text{LL}}^\ell = 0, \end{aligned} \quad (\text{A.5})$$

i.e., according to (2.4)

$$\frac{1}{x} F_{2, \text{box}}^\ell(x, Q^2) = 3 \Sigma e_q^4 \frac{\alpha}{\pi} \left\{ [x^2 + (1-x)^2] \ln \frac{Q^2(1-x)}{m_q^2 x} + 8x(1-x) - 1 \right\}. \quad (\text{A.6})$$

The heavy quark contribution becomes

$$\begin{aligned} F_{\text{TT}}^h &= 3 e_h^4 \frac{\alpha}{\pi} \theta(\beta^2) \left\{ \left[ x^2 + (1-x)^2 + x(1-x) \frac{4m_h^2}{Q^2} - x^2 \frac{8m_h^4}{Q^4} \right] \ln \frac{1+\beta}{1-\beta} \right. \\ &\quad \left. + \beta \left[ 4x(1-x) - 1 - x(1-x) \frac{4m_h^2}{Q^2} \right] \right\} \\ F_{\text{LT}}^h &= 3 e_h^4 \frac{\alpha}{\pi} \theta(\beta^2) \left\{ -x^2 \frac{8m_h^2}{Q^2} \ln \frac{1+\beta}{1-\beta} + \beta [4x(1-x)] \right\} \\ F_{\text{TL}}^h &= F_{\text{LL}}^h = 0, \end{aligned} \quad (\text{A.7})$$

i.e., according to (2.4),

$$\begin{aligned} \frac{1}{x} F_{2, \text{box}}^h(x, Q^2) &= 3 e_h^4 \frac{\alpha}{\pi} \theta(\beta^2) \left\{ \left[ x^2 + (1-x)^2 + x(1-x) \frac{4m_h^2}{Q^2} \right. \right. \\ &\quad \left. \left. - x^2 \frac{8m_h^4}{Q^4} \right] \ln \frac{1+\beta}{1-\beta} + \beta \left[ 8x(1-x) - 1 - x(1-x) \frac{4m_h^2}{Q^2} \right] \right\} \end{aligned} \quad (\text{A.8})$$

and  $\frac{1}{x} F_{\text{L, box}}^h(x, Q^2) = F_{\text{LT}}^h$ , which are the familiar massive Bethe–Heitler expressions [22] relevant for the heavy quark contributions to the structure functions of real photons (cf. [9], for example).

## References

- [1] C. Adloff et al., H1 Collab., *Eur. Phys. J.* **C13**, 397 (2000).
- [2] M. Acciarri et al., L3 Collab., *Phys. Lett.* **B483**, 373 (2000).
- [3] T. Uematsu and T.F. Walsh *Phys. Lett.* **101B**, 263 (1981); *Nucl. Phys.* **B199**, 93 (1982); W. Ibes and T.F. Walsh, *Phys. Lett.* **B251**, 450 (1990).
- [4] G. Rossi, *Phys. Rev.* **D29**, 852 (1984); UC San Diego report UCDS-10P10-227 (1983), unpublished.
- [5] F.M. Borzumati and G.A. Schuler, *Z. Phys.* **C58**, 139 (1993).
- [6] M. Glück, E. Reya, and M. Stratmann, *Phys. Rev.* **D51**, 3220 (1995).
- [7] G.A. Schuler and T. Sjöstrand, *Z. Phys.* **C68**, 607 (1995); *Phys. Lett.* **B376**, 193 (1996).
- [8] M. Drees and R.M. Godbole, *Phys. Rev.* **D50**, 3124 (1994).
- [9] M. Glück, E. Reya, and I. Schienbein, *Phys. Rev.* **D60**, 054019 (1999); **62**, 019902 (2000)(E).
- [10] M. Erdmann, ‘The Partonic Structure of the Photon’, Springer Tracts in Modern Physics **138** (1997).
- [11] R. Nisius, *Phys. Rep.* **332**, 165 (2000).
- [12] V.M. Budnev, I.F. Ginzburg, G.V. Meledin, and V.G. Serbo, *Phys. Rep.* **15**, 181 (1975).
- [13] Ch. Berger and W. Wagner, *Phys. Rep.* **146**, 1 (1987).
- [14] Ch. Berger et al., PLUTO Collab., *Phys. Lett.* **142B**, 119 (1984).



- [15] T.F. Walsh and P. Zerwas, *Phys. Lett.* **44B**, 195 (1973);  
C. Peterson, T.F. Walsh, and P. Zerwas, *Nucl. Phys.* **B174**, 424 (1980).
- [16] S. Frixione, M.L. Mangano, P. Nason, and G. Ridolfi, *Phys. Lett.* **B319**, 339 (1993).
- [17] M. Glück, E. Reya, and A. Vogt, *Eur. Phys. J.* **C5**, 461 (1998).
- [18] J. Chyla, *Phys. Lett.* **B488**, 289 (2000);  
J. Chyla and M. Tasevsky, *Eur. Phys. J.* **C16**, 471 (2000).
- [19] B.V. Combridge and C.J. Maxwell, *Nucl. Phys.* **B239**, 429 (1984).
- [20] M. Klasen, G. Kramer, and B. Pötter, *Eur. Phys. J.* **C1**, 261 (1998);  
G. Kramer and B. Pötter, *Eur. Phys. J.* **C5**, 665 (1998);  
B. Pötter, *Comp. Phys. Comm.* **119**, 45 (1999); DESY 97–138 (Ph.D. thesis, unpublished).
- [21] M. Glück, E. Reya and M. Stratmann, *Phys. Rev.* **D54**, 5515 (1996).
- [22] E. Witten, *Nucl. Phys.* **B104**, 445 (1976);  
M. Glück and E. Reya, *Phys. Lett.* **83B**, 98 (1979).

## Figure Captions

**Fig. 1** Predictions for  $F_{\text{eff}}$  as defined in (2.3). The light ( $u, d, s$ ) and heavy (charm) contributions in (2.5) of the ‘full box’ expressions in (A.1) – (A.4) are calculated as explained in the text below eq. (2.5). The ‘asymptotic box’ results refer to the light quark contributions being given by (2.6) or (2.7) and (2.8). The QCD resummed NLO expectations of GRS [9] for  $F_2$  in (3.4) turn out to be similar to the LO ones [9]. Also shown are the LO–resummed results of SaS 1D [7] for  $F_2$  and  $F_{\text{eff}} = F_2 + \frac{3}{2} F_{\text{LT}}$  as discussed in Sec. 3. The total charm contribution to the latter two QCD results involves also a ‘resolved’ component, e.g., eqs. (3.2) and (3.3), which turns out to be small as compared to the box contribution shown which dominates in the kinematic region considered. The PLUTO data are taken from [14].

**Fig. 2** As in fig. 1, but for  $Q^2 = 120 \text{ GeV}^2$  and  $P^2 = 3.7 \text{ GeV}^2$  appropriate for the LEP–L3 data [2].

**Fig. 3** Predictions for the effective parton density defined in eq. (5.1). The ‘box’ results refer to the universal  $q_{\text{box}}^{\gamma(P^2)}$  in (2.10), and the ‘effective’ ones to  $q_{\text{eff}}^{\gamma(P^2)}$  as defined in (5.2) as derived from the full box expressions (A.1) – (A.4) including all  $\mathcal{O}(P^2/Q^2)$  contributions. The LO–QCD predictions of GRS [9] are shown by the solid curves which refer to the predictions in the theoretically legitimate region  $P^2 \ll Q^2$ , whereas the dashed curves extend into the kinematic region of larger  $P^2$  approaching  $Q^2$  where the concept of QCD–resummed parton distributions of virtual photons is not valid anymore. (Note that the results for  $x = 0.6$  terminate at  $P^2 \simeq 54 \text{ GeV}^2$  due to the kinematic constraint  $W^2 > 0$ , with  $W^2$  being defined below (A.4), i.e.  $x < (1 + P^2/Q^2)^{-1}$ .) For illustration we also show the effective LO–QCD parton density  $\tilde{f}^\gamma$  of a real photon  $\gamma \equiv \gamma(P^2 = 0)$  of GRS [9] multiplied by the simple  $\rho$ –pole suppression factor  $\eta(P^2)$  in (3.5) which clearly underestimates the H1–data [1].

**Fig. 4** Expected charm contributions to  $F_2$ . The naive ‘direct (box)’ result refers to  $F_{2,\text{box}}^c$  in (3.2) and the LO–QCD ‘resolved’ prediction is due to  $F_{2,g^{\gamma(P^2)}}^c$  in (3.2), as explicitly given in (3.3) with  $g^{\gamma(P^2)}(x, 4m_c^2)$  taken from GRS [9]. This latter ‘resolved’ contribution is absent in the naive box (QPM) approach.

**Fig. 5** Predictions for the total light quark  $\Sigma^{\gamma(P^2)} \equiv 2\Sigma_{q=u,d,s} q^{\gamma(P^2)}$  and gluon contributions to the effective parton density in (5.1) at a fixed scale  $Q^2 = 85 \text{ GeV}^2$  and two fixed virtualities  $P^2 = 1$  and  $5 \text{ GeV}^2$ . The naive box results refer to the universal  $q_{\text{box}}^{\gamma(P^2)}$  defined in (2.10), and to  $q_{\text{eff}}^{\gamma(P^2)}$  defined in (5.2). The LO–QCD RG–resummed predictions are denoted by  $\Sigma^{\gamma(P^2)}$  and  $g^{\gamma(P^2)}$  according to GRS [9]. The latter gluon contribution is absent in the naive box (QPM) approach.

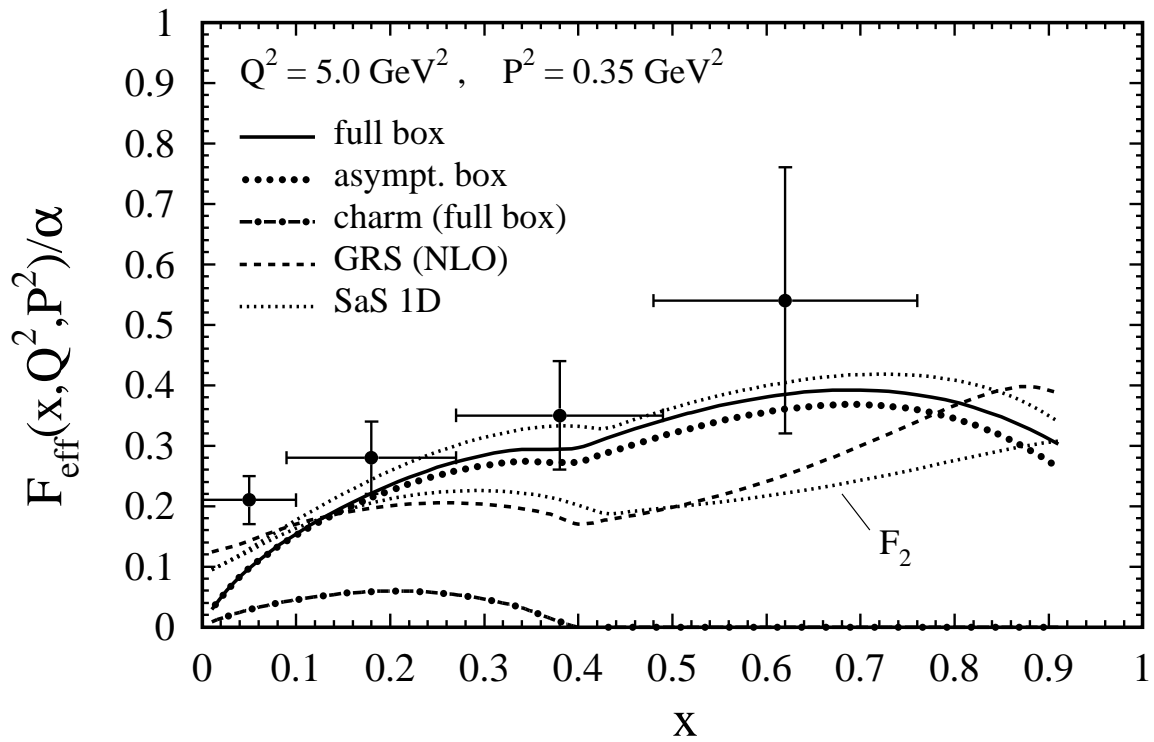


Fig. 1

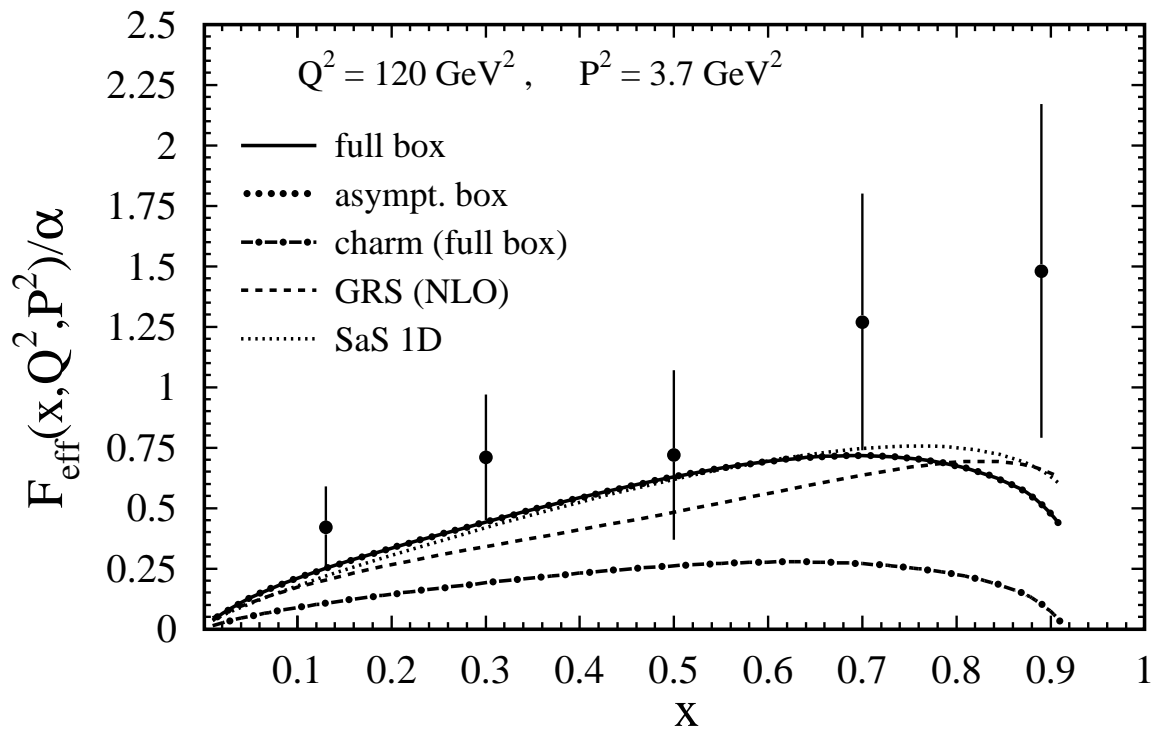


Fig. 2

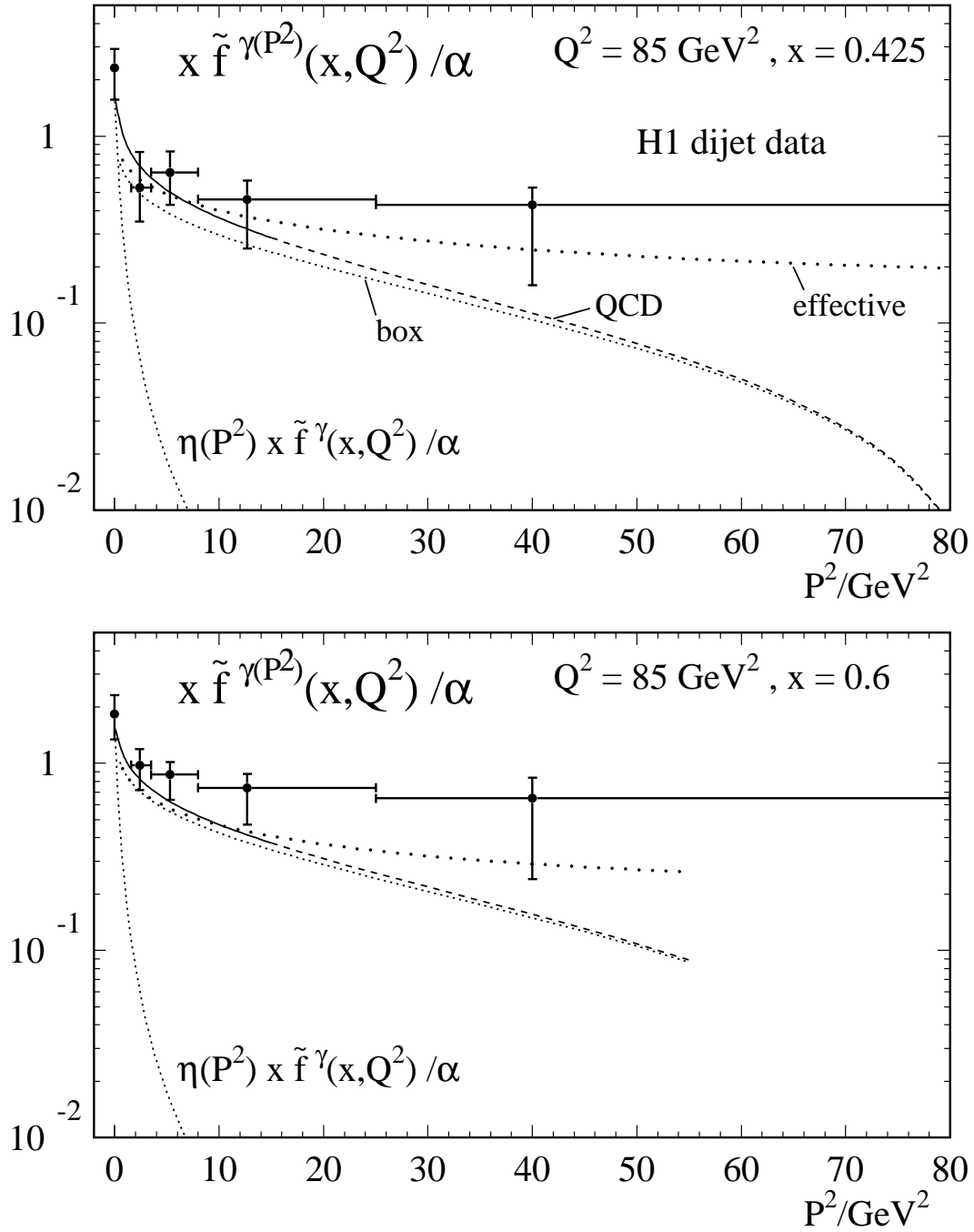


Fig. 3

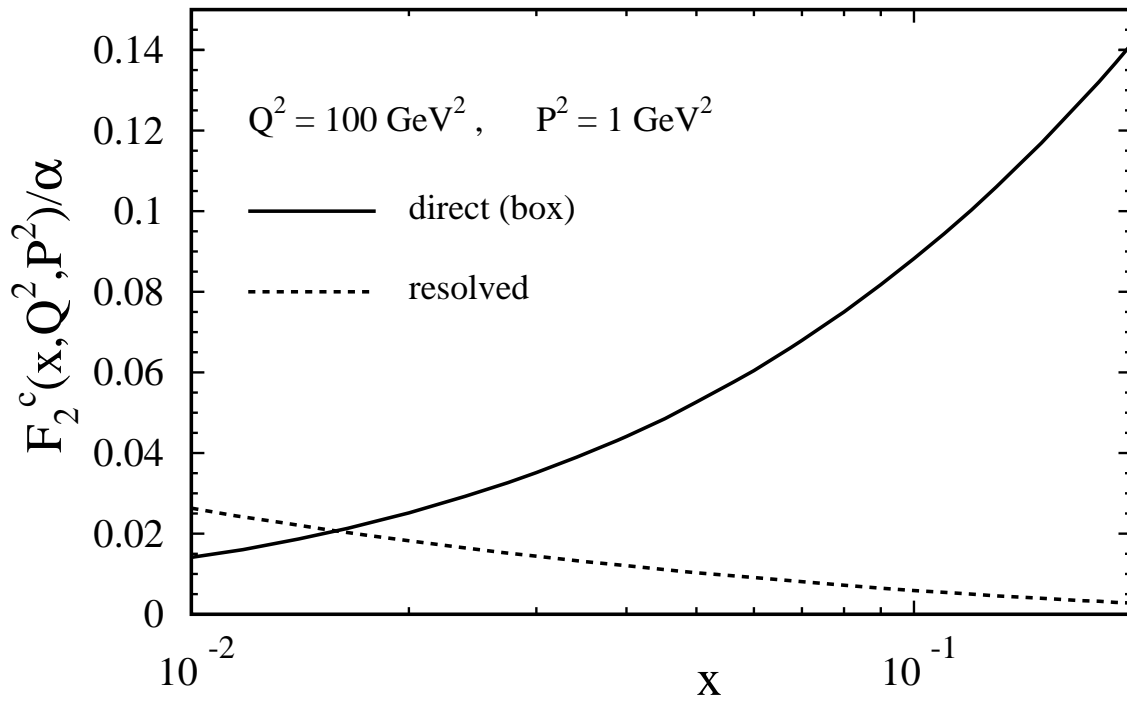


Fig. 4

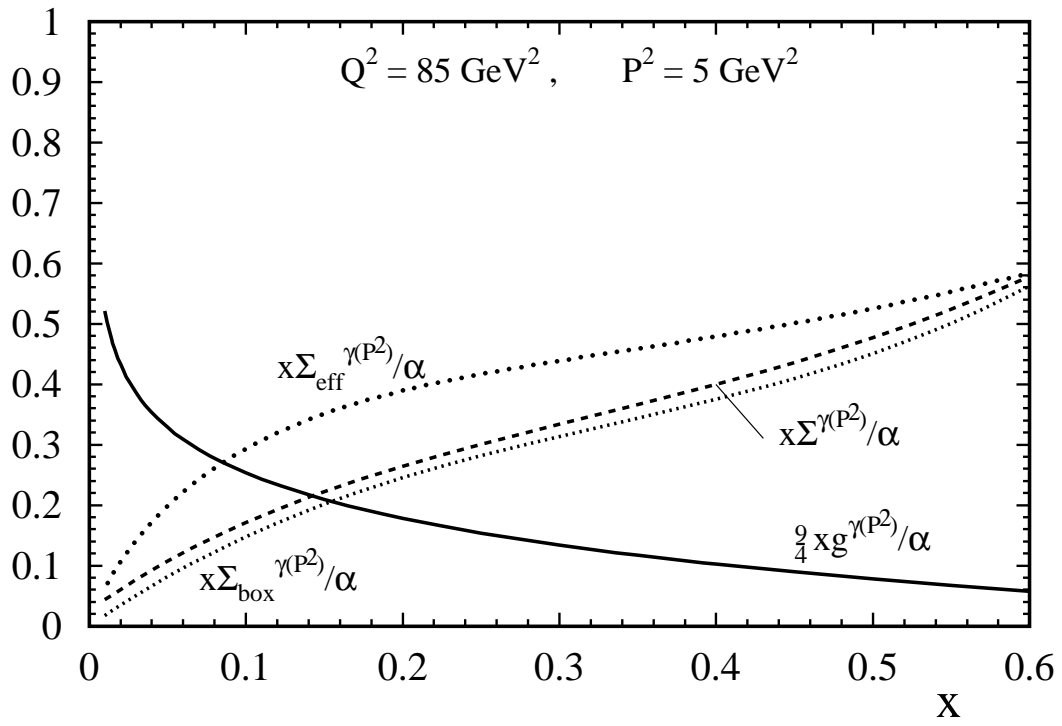
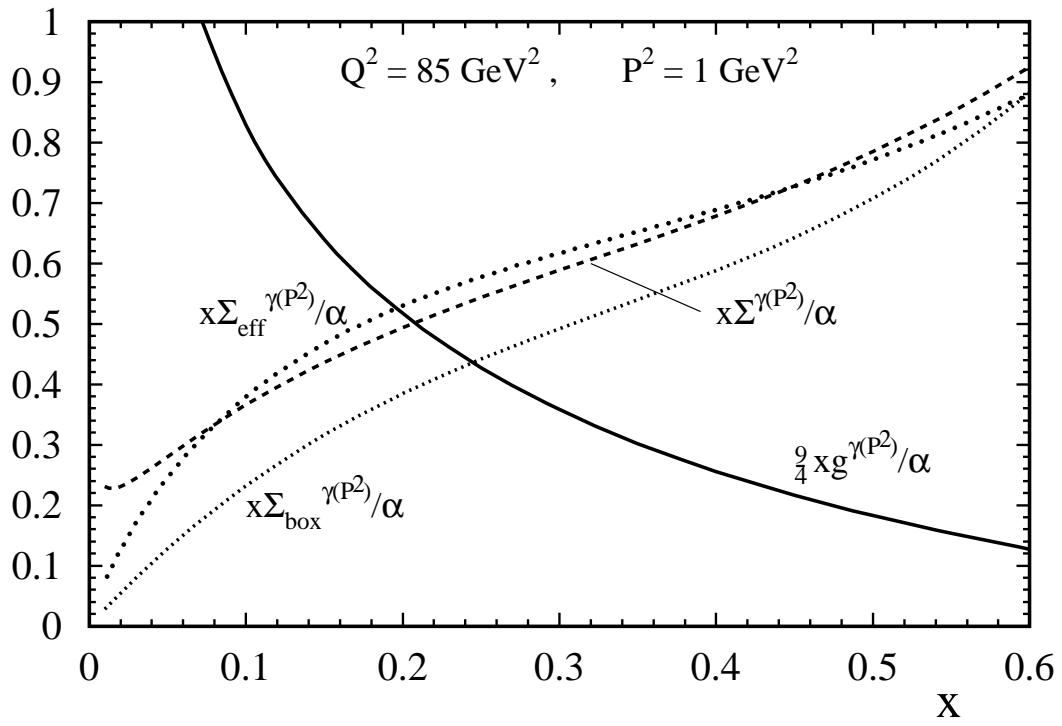


Fig. 5